Numerical Simulation and Control of Robot Welding Deformation of Five-Port Connector

Chen hua-bin, Xu Tao, Chen Shan-ben, and Lin Tao

Institute of Welding, School of Materials Science and Engineering, Shanghai Jiaotong University, Shanghai 200030, China
hbchen@sjtu.edu.cn

Abstract. The unfitness of weld and gap variation are salient using traditional TIG procedure for the five-port connector flange. Insufficient reliability and the instability of the weld are catastrophe, which cannot accommodate to new generation type production's requirement. In this study, a finite element model of the five-port connector was built and the distribution of temperature field and deformation were studied. The result shows that welding thermal cycle is greatly different from the ordinary butt weld during welding of the flange and spherical shell. The welding deformation is complex from the direction of UX and UZ. Especially maximum deformation from the direction of UZ is about 4.96mm .According to the result, the optimum welding fixture is designed on the view of the smallest deformation, to critically control the deformation of the both sides of the welding line, finally to accomplish the robotic flexible welding.

1 Introduction

In the spaceflight industry, thin-walled structure occupy sizable proportion，which belongs to important component. Because of non-uniform thermal expansion and shrinkage，Deformations of a welded work-piece would be occurred, then directly affected manufacturing quality and service deadline of the welding product [1-3]. If the distortion of the structure can be predicted accurately for the complex weld, the optimum welding fixture and procedure scheme is designed on the view of the smallest deformation. It can greatly improve efficiency and critically control the welding deformation of the both sides. However, how to predict and control the welding deformation has become an urgent problem further [4-8].

In this paper, thermal elastic-plastic FEM (Finite-Element-Method) was used to analyze the five-port connector of the rocket. At the same time, the accuracy and iterative convergence speed, which occurred in dealing with the complex, weld structure, corresponding material attribute reduction and computation techniques had been improved. The optimum welding procedure scheme is designed on the view of the smallest deformation, which satisfied the accurate prediction and controlling for the arc welding.

T.-J. Tarn et al. (Eds.): Robot. Weld., Intellige. & Automation, LNCIS 362, pp. 203–209, 2007.
springerlink.com

2 Model of the Flange Weld

2.1 Finite Element Model

In the numerical simulation of the five-port connector for LF12 aluminum alloy, it is assumed that the base metal is the same as the welding materials during welding. The spherical shell is 450mm in diameter, 3mm in thickness, in which uniformly distribute four flange holes along the radial direction of 38°（Fig.1）. The flange hole is 180mm in diameter, which weld by one side. The AC ampere and voltage used for welding were 150A and 15V.

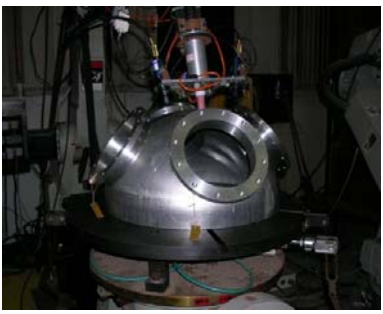

Fig. 1. Five-port connector used in experiment

In this paper, hemispheric Gauss thermal model was adopted. Equation(1)can be represented GTAW moving thermal model. Where Q is the instant heat applied to the work piece; x,y,z are the half axis.

$$q(x,y,z)=\frac{6\sqrt{3}Q}{\pi^{3/2}abc}\exp(-3(\frac{x^2}{a^2}+\frac{y^2}{b^2}+\frac{z^2}{c^2})) \tag{1}$$

During welding process, elastic-plastic deformation would be occurred according to the equation(2).The relations between displacement $\{d\delta\}$ and strain $\{d\varepsilon\}^e$ increment are shown as follows:

$$\{d\varepsilon\}^e=[\mathrm{B}]\{d\delta\}^e \tag{2}$$

where [B] is the elastic-plastic matrix，which is related with the linear expansion coefficient and yield strength [9].

2.2 The Material Properties

The reliability of material properties should be validated. According to the above discussion, part of the adoptive parameter is quoted from the document [10-11]. The properties at elevated temperatures are obtained by through bilinear interpolation in this paper.

Figure 2 shows a simulated model. A computational model using a finite difference analysis was appropriately modified to investigate the reliability of the material properties. Using RS232C universal meter, the temperature in the HAZ was measured with special designed USB interface. Numerical calculations were consistent with the measured value.

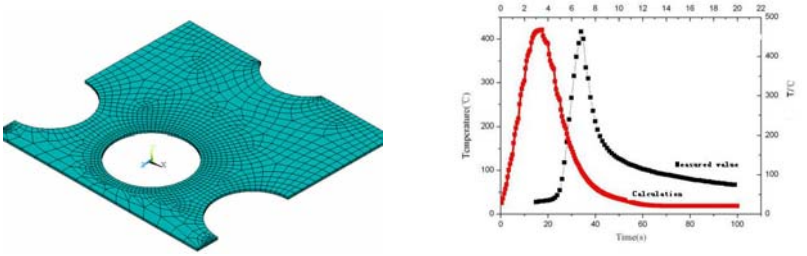

Fig. 2. Model of sample in ANSYS and comparison of temperature between calculations and measured value

3 Simulation Result of the Welding Process

3.1 Simulation Result of the Welding Temperature Field

Fig.3 shows dynamic three-dimensional temperature field of 1s and 10s.From the distribution of the temperature field, the weld temperature field varied from the moving heat source. Owing to the difference of the boundary condition for heat dissipation, peak temperature will continuously change. When loading time is at 1s, the temperature of the local weld is very high and the gradient is also great. The result is similar to the actual welding process. When the heat source moved, heat dissipation for the flange hole is contributed to the badly heat-dispersed condition. As a consequence, the loading time is conducted at 10s, which make the temperature gradient maximum. Considering the thermal conduction, the heat transfer between work-piece and atmosphere, weld metal undergo the rapid heat rating.

In the numerical model, three test points on the spherical shell were chosen to study how to recognize the happening of the local temperature distribution. These points were chosen at the different location of the weld. Figure 4 represents the thermal recycle curve between calculation and measured value. The varied trend of temperature is uniformed.

From the above-mentioned simulation results, the peak temperature of the weld zoon is occurred at the position of the badly heat-dispersed condition. Because of the superposition of the arc starting and end welding, the initial welding position undergoes twice obvious thermal recycle.

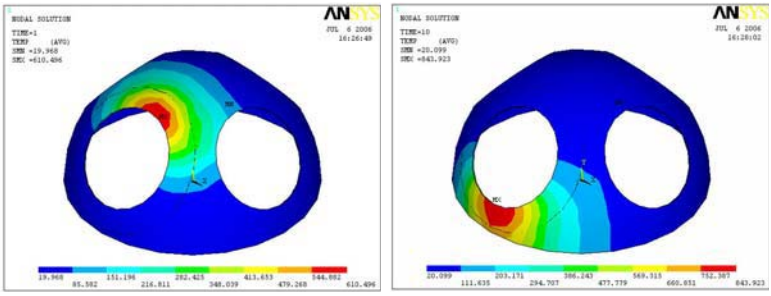

Fig. 3. Distribution of temperature field

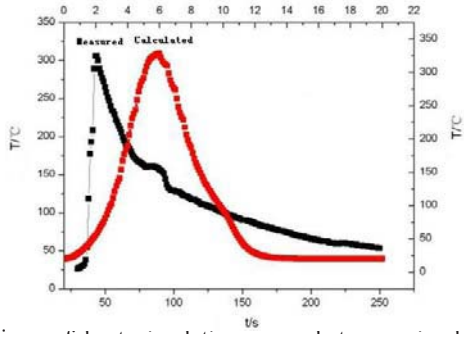

Fig. 4. Comparison of heat circulation curve between simulation of welding five-port connector and experimentation

3.2 Simulation Result of the Welding Deformation

A non-linear transient thermal analysis is performed to predict the temperature history of the whole domain. In order to ensure correct loading, the finite element model for both thermal and structural analysis is the same except for element type.

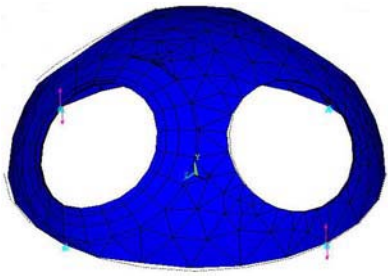

Fig. 5. Welding deformation of spherical shell

For structural analysis the element type is the SOLID45. with three translational degrees of freedom a t each node.The results of the thermal analysis are applied as a thermal body load in a non-linear transient structural analysis to calculate deformation and stresses. The minimal step is set to 0.0001s. According to the simulation of the result, thermoplastic behavior was analyzed. Especially, the whole structure from the direction of UX and UZ was conducted under the free condition. In order to investigate the deformation, 2-time magnification was used to the model.

It can be seen from Fig.5 that there is an obvious deformation in or near the flange weld. Dash line indicates non-deformed profile. The uneven contraction appears along the radial direction of the flange hole. Because of the different thickness between spherical shell and flange, the distribution of the residual plastic strain is asymmetric. Consequently, there will be elliptical deformation on the flange hole. Results of axial displacement (UZ) on the flange hole from the radial direction have been testified. These asymmetric residual compressive stresses cause axial displacement near the weldment.

In Fig.6, the axial displacement for the UZ direction that is located on the weldment. From the figure, it can be easily seen that there is a jump in the deformation diagrams in points No.2. The magnitude of the jump in the c with the further decrease in temperature, the plastic deformation reduces 0.77mm after the elastic limit. The magnitude of the deformation is relative low in the weld start position owing to the restrain from the top spherical shell. It is observed that there is twice elastic deformation in the initiation arc.

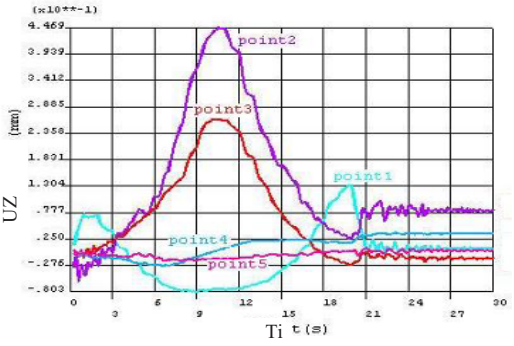

Fig. 6. UZ displacement

In the experiment contraction appears and the maximum deformation measured 1.0mm in the bottom spherical shell (Fig.7). The flatness of the bottom spherical shell indicated “M” in shape. The residual compressive stresses cause contraction in the flange hole along the radial direction.

According to the simulation result of the five-port connector, controlling the deformation from two aspects follows as: (1) the adjustment of the welding procedure ; (2)the design of the optimum welding fixture on the view of the smallest deformation.

As the arc proceeds, the welding gap varied constantly due to the contraction of the solidifying welding bead. The flange weld is divided into four sections and the welding sequence follows as Fig.8.

The design scheme of “Sandwich” type will be applied to the welding process device. It is directly fixed on the robot modified gear. While the spherical manipulator would be used to push against the inner surface of the spherical shell, it could be controlling the contraction.

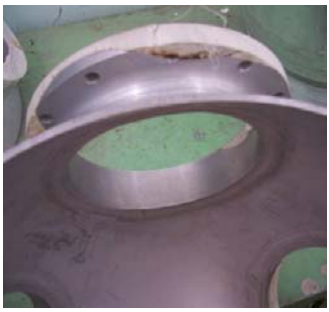

Fig. 7. Workpiece of five-port connector

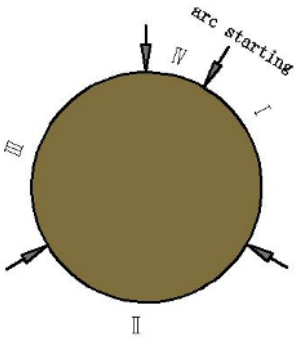

Fig. 8. Welding sequence

4 Conclusions

This model is useful to study the thermal and mechanical behaviors of structures during the welding process, and also is useful to optimize the welding procedure.

1) The initial welding position undergone twice obvious thermal recycle that is different to conventional butt welding. The great temperature gradient appeared on the bottom of the spherical shell.

2) During welding proceed, the distribution of the temperature field varied constantly owing to the differential heat dissipation boundary condition and resulted in the asymmetric residual stressed distribution. Tensile stress occurred around the weld and the compressive stresses were produced on bottom of the spherical shell.

3) The maximum elastic deformation for point No. 2 is 4.96 mm, which is just identical with actual welding process. In order to critically control the deformation of the both sides of the welding line, the design scheme of “Sandwich” type is applied to the welding process device.

Acknowledgements

This work is supported by Key Foundation Program of Shanghai Sciences & Technology Committee under Grand No. 06JC14036 and the Key Foundation Program of Shanghai Sciences & Technology Committee under Grant No. 06JC14036.

References

1. C.L. Tsai, S.C.Park, W.T. Cheng, Welding distortion of a thin-plate panel structure ,Weld.J., Res.Suppl.1999(78):156s-165s.
2. Lin YC, Chou CP. A new technique for reduction of residual stress induced by welding in type 304 stainless steel. J Mater Process Technol 1995;48:693–8.
3. Goldak J, Chakravarti A, Bibby M. A new finite element model for welding heat sources. Metall Trans B 1984;15B: 299–305.
4. V. Kamala, J.A. Goldak, Error due to two dimensional approximations in heat transfer analysis of welds, Weld. J. 76 (9) (1993) 440s–446s.
5. Goldak J, ChakravartA, BibbyM. A new finite element model for welding heat source[J]. Metallurgical TransactionsB, 1984, 15 : 299 – 305.
6. Lindgren LE, Hedblom R. Modeling of addition of filler material in large deformation analysis of multipass welding. Common Number Methods Eng 2001;17:647–57.
7. Lindgren LE. Finite Element Modeling and Simulation of Welding Part 1: Increased complexity. J Therm Stress 2001;24:141–92.
8. Tso-Liang Teng, Peng-Hsiang Chang, Hsush-Chao Koc. Finite element analysis of circular patch welds[J]. International Journal of Pressure Vessels and Piping, 2000,7(11): 643-650.
9. Andersen, L., Residual Stresses and Deformations in Steel Structures, PhD. thesis, Technical University of Denmark, 2000.
10. Goldak J, Bibby M, Moore J, House R, Patel B. Computer modeling of heat flow in welds. Metall Trans B 1985;17B:587–600.
11. M.R. Nami, M.H. Kadivar, K. Jafarpur, Three-dimensional thermal response of thick plate weldments: Effect of layer-wise and piecewise welding, Model. Simul. Mater. Sci. Eng. 12 (2004) 731–743.